Amendment to the Claims:

Cancel Claims 51 and 52.

Amend Claim 49.

Listing of Claims:

1. (original) A dihydrogenphosphate salt of (2*R*)-4-oxo-4-[3-(trifluoromethyl)-5,6-dihydro[1,2,4]triazolo[4,3-*a*]pyrazin-7(8*H*)-yl]-1-(2,4,5-trifluorophenyl)butan-2-amine of structural formula I:

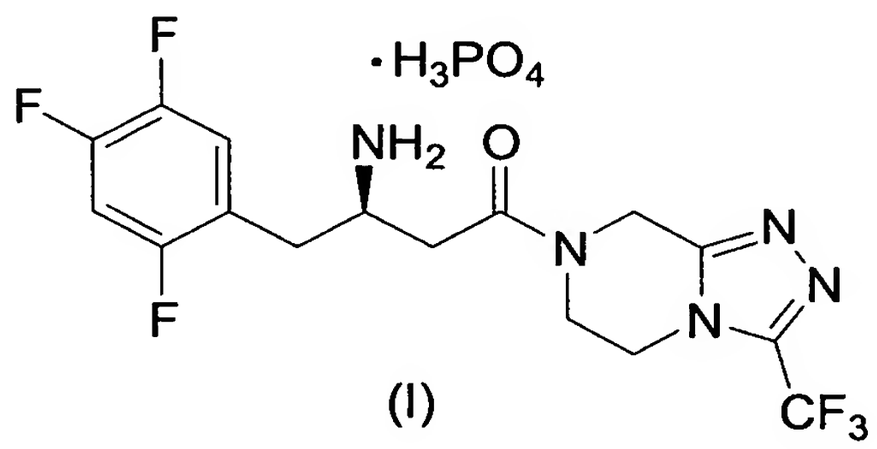

(I)

characterized as being a crystalline anhydrate Form I.

2. (original) The crystalline anhydrate Form I of Claim 1 characterized by characteristic reflections obtained from the X-ray powder diffraction pattern at spectral d-spacings of 18.42, 9.35, and 6.26 angstroms.

3. (original) The crystalline anhydrate Form I of Claim 2 further characterized by characteristic reflections obtained from the X-ray powder diffraction pattern at spectral d-spacings of 5.78, 4.71, and 3.67 angstroms.

4. (original) The crystalline anhydrate Form I of Claim 3 further characterized by characteristic reflections obtained from the X-ray powder diffraction pattern at spectral d-spacings of 3.99, 2.71, and 2.66 angstroms.

5. (original) The crystalline anhydrate Form I of Claim 4 further characterized by the X-ray powder diffraction pattern of FIG. 1.

6. (original) The crystalline anhydrate Form I of Claim 1 characterized by a solid-state fluorine-19 MAS nuclear magnetic resonance spectrum showing signals at -65.3, -105.1, and -120.4 p.p.m.

7. (original) The crystalline anhydrate Form I of Claim 6 further characterized by a solid-state fluorine-19 MAS nuclear magnetic resonance spectrum showing signals at -80.6, -93.5, and -133.3 p.p.m.

8. (original) The crystalline anhydrate Form I of Claim 7 further characterized by the solid-state fluorine-19 MAS nuclear magnetic resonance spectrum of FIG. 3.

9. (original) The crystalline anhydrate Form I of Claim 1 characterized by the solid-state carbon-13 CPMAS nuclear magnetic resonance spectrum of FIG. 2.

10. (original) The crystalline anhydrate Form I of Claim 1 characterized by the thermogravimetric analysis curve of FIG. 5.

11. (original) The crystalline anhydrate Form I of Claim 1 characterized by the differential scanning calorimetric (DSC) curve of FIG. 4.

12. (original) A dihydrogenphosphate salt of (2*R*)-4-oxo-4-[3-(trifluoromethyl)-5,6-dihydro[1,2,4]triazolo[4,3-*a*]pyrazin-7(8*H*)-yl]-1-(2,4,5-trifluorophenyl)butan-2-amine of structural formula I:

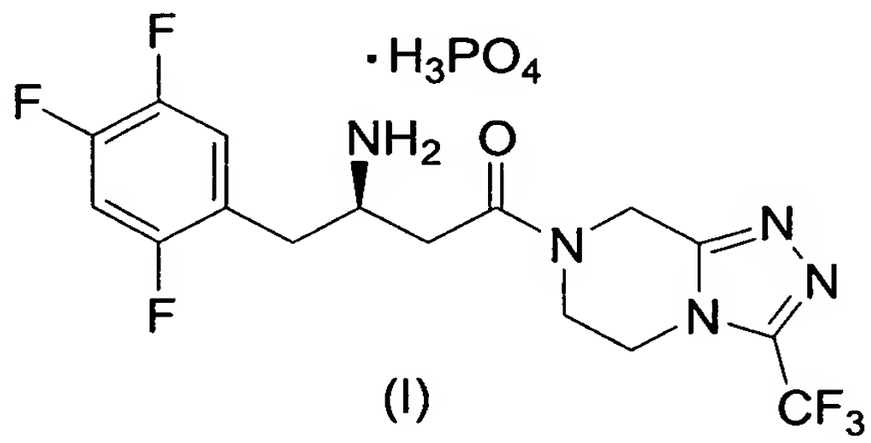

(I)

characterized as being a crystalline anhydrate Form III.

13. (original) The crystalline anhydrate Form III of Claim 12 characterized by characteristic reflections obtained from the X-ray powder diffraction pattern at spectral d-spacings of 17.88, 6.06, and 4.26 angstroms.

14. (original) The crystalline anhydrate Form III of Claim 13 further characterized by characteristic reflections obtained from the X-ray powder diffraction pattern at spectral d-spacings of 9.06, 5.71, and 4.55 angstroms.

15. (original) The crystalline anhydrate Form III of Claim 14 further characterized by characteristic reflections obtained from the X-ray powder diffraction pattern at spectral d-spacings of 13.69, 6.50, and 3.04 angstroms.

16. (original) The crystalline anhydrate Form III of Claim 15 further characterized by the X-ray powder diffraction pattern of FIG. 11.

17. (original) The crystalline anhydrate Form III of Claim 12 characterized by a solid-state fluorine-19 MAS nuclear magnetic resonance spectrum showing signals at -63.0, -103.1, and -120.2 p.p.m.

18. (original) The crystalline anhydrate Form III of Claim 17 further characterized by a solid-state fluorine-19 MAS nuclear magnetic resonance spectrum showing signals at -95.3, -98.7, -135.2, and -144.0 p.p.m.

19. (original) The crystalline anhydrate Form III of Claim 18 further characterized by the solid-state fluorine-19 MAS nuclear magnetic resonance spectrum of FIG. 13.

20. (original) The crystalline anhydrate Form III of Claim 12 characterized by the solid-state carbon-13 CPMAS nuclear magnetic resonance spectrum of FIG. 12.

21. (original) The crystalline anhydrate Form III of Claim 12 characterized by the thermogravimetric analysis curve of FIG. 15.

22. (original) The crystalline anhydrate Form III of Claim 12 characterized by the differential scanning calorimetric (DSC) curve of FIG. 14.

23. (original) A dihydrogenphosphate salt of (2*R*)-4-oxo-4-[3-(trifluoromethyl)-5,6-dihydro[1,2,4]triazolo[4,3-*a*]pyrazin-7(8*H*)-yl]-1-(2,4,5-trifluorophenyl)butan-2-amine of structural formula I:

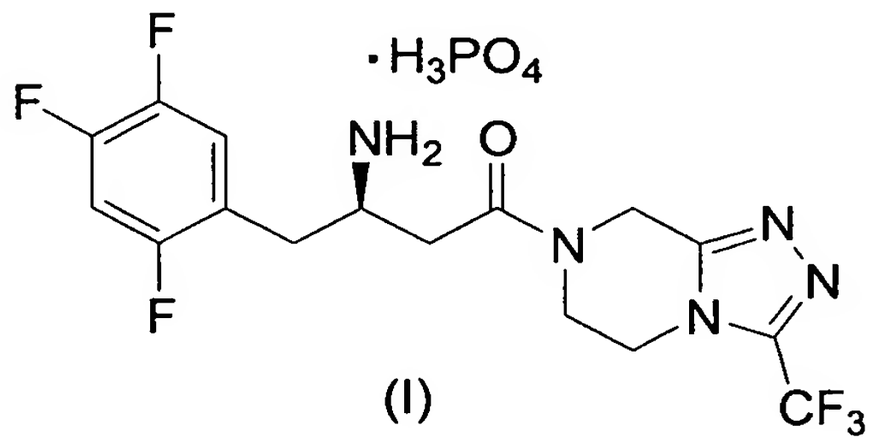

(I)

characterized as being a crystalline desolvated anhydrate Form II.

24. (original) The crystalline desolvated anhydrate Form II of Claim 23 characterized by characteristic reflections obtained from the X-ray powder diffraction pattern at spectral d-spacings of 7.09, 5.27, and 4.30 angstroms.

25. (original) The crystalline desolvated anhydrate Form II of Claim 24 further characterized by characteristic reflections obtained from the X-ray powder diffraction pattern at spectral d-spacings of 18.56, 9.43, and 4.19 angstroms.

26. (original) The crystalline desolvated anhydrate Form II of Claim 25 further characterized by characteristic reflections obtained from the X-ray powder diffraction pattern at spectral d-spacings of 6.32, 5.82, and 3.69 angstroms.

27. (original) The crystalline desolvated anhydrate Form II of Claim 26 further characterized by the X-ray powder diffraction pattern of FIG. 6.

28. (original) The crystalline desolvated anhydrate Form II of Claim 23 characterized by a solid-state fluorine-19 MAS nuclear magnetic resonance spectrum showing signals at -65.1, -104.9, and -120.1 p.p.m.

29. (original) The crystalline desolvated anhydrate Form II of Claim 28 further characterized by a solid-state fluorine-19 MAS nuclear magnetic resonance spectrum showing signals at -80.3, -94.5, -134.4, and -143.3 p.p.m.

30. (original) The crystalline desolvated anhydrate Form II of Claim 29 further characterized by the solid-state fluorine-19 MAS nuclear magnetic resonance spectrum of FIG. 8.

31. (original) The crystalline desolvated anhydrate Form II of Claim 23 characterized by the solid-state carbon-13 CPMAS nuclear magnetic resonance spectrum of FIG. 7.

32. (original) The crystalline desolvated anhydrate Form II of Claim 23 characterized by the thermogravimetric analysis curve of FIG. 10.

33. (original) The crystalline desolvated anhydrate Form II of Claim 23 characterized by the differential scanning calorimetric (DSC) curve of FIG. 9.

34. (original) A dihydrogenphosphate salt of (2*R*)-4-oxo-4-[3-(trifluoromethyl)-5,6-dihydro[1,2,4]triazolo[4,3-*a*]pyrazin-7(8*H*)-yl]-1-(2,4,5-trifluorophenyl)butan-2-amine of structural formula I:

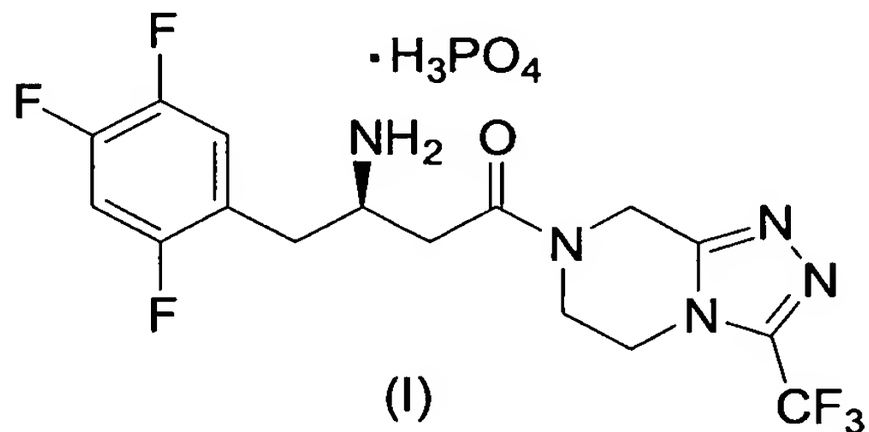

(I) ;

characterized as being a crystalline solvate wherein the solvate is selected from the group consisting of acetone solvate, acetonitrile solvate, methanolate, ethanolate, 1-propanolate, and 2-propanolate.

35. (original) The crystalline solvate of Claim 34 wherein said solvate is an ethanolate.

36. (original) The crystalline ethanolate of Claim 35 characterized by characteristic reflections obtained from the X-ray powder diffraction pattern at spectral d-spacings of 7.09, 5.27, and 4.30 angstroms.

37. (original) The crystalline ethanolate of Claim 36 further characterized by characteristic reflections obtained from the X-ray powder diffraction pattern at spectral d-spacings of 18.56, 9.43, and 4.19 angstroms.

38. (original) The crystalline ethanolate of Claim 37 further characterized by characteristic reflections obtained from the X-ray powder diffraction pattern at spectral d-spacings of 6.32, 5.82, and 3.69 angstroms.

39. (original) The crystalline ethanolate of Claim 38 further characterized by the X-ray powder diffraction pattern of FIG. 16.

40. (original) The crystalline ethanolate of Claim 35 characterized by a solid-state fluorine-19 MAS nuclear magnetic resonance spectrum showing signals at -64.7, -104.5, and -121.9 p.p.m.

41. (original) The crystalline ethanolate of Claim 40 further characterized by a solid-state fluorine-19 MAS nuclear magnetic resonance spectrum showing signals at -94.3, -117.7, -131.2, and -142.6 p.p.m.

42. (original) The crystalline ethanolate of Claim 41 further characterized by the solid-state fluorine-19 MAS nuclear magnetic resonance spectrum of FIG. 18.

43. (original) The crystalline ethanolate of Claim 35 characterized by the solid-state carbon-13 CPMAS nuclear magnetic resonance spectrum of FIG. 17.

44. (original) The crystalline ethanolate of Claim 35 characterized by the thermogravimetric analysis curve of FIG. 20.

45. (original) The crystalline ethanolate of Claim 35 characterized by the differential scanning calorimetric (DSC) curve of FIG. 19.

46. (original) A drug substance which is the dihydrogenphosphate salt of (2*R*)-4-oxo-4-[3-(trifluoromethyl)-5,6-dihydro[1,2,4]triazolo[4,3-*a*]pyrazin-7(8*H*)-yl]-1-(2,4,5-trifluorophenyl)butan-2-amine of structural formula I:

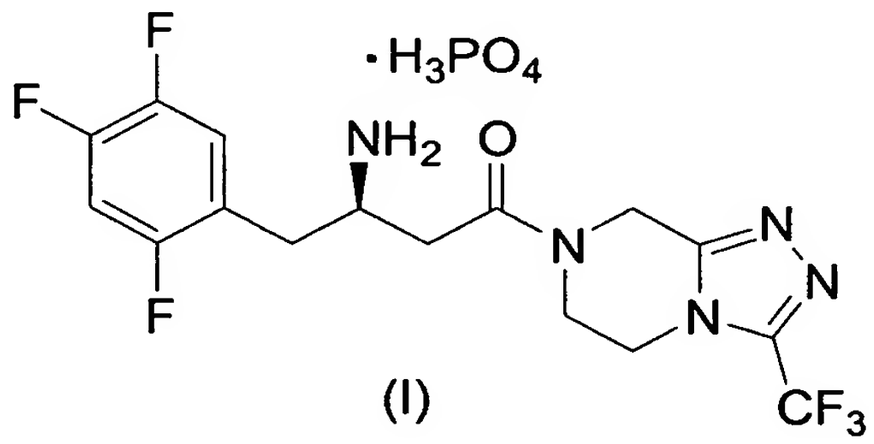

(I)

comprising a mixture of crystalline anhydrate Form I and crystalline anhydrate Form III.

47. (original) A dihydrogenphosphate salt of (2*R*)-4-oxo-4-[3-(trifluoromethyl)-5,6-dihydro[1,2,4]triazolo[4,3-*a*]pyrazin-7(8*H*)-yl]-1-(2,4,5-trifluorophenyl)butan-2-amine of structural formula I:

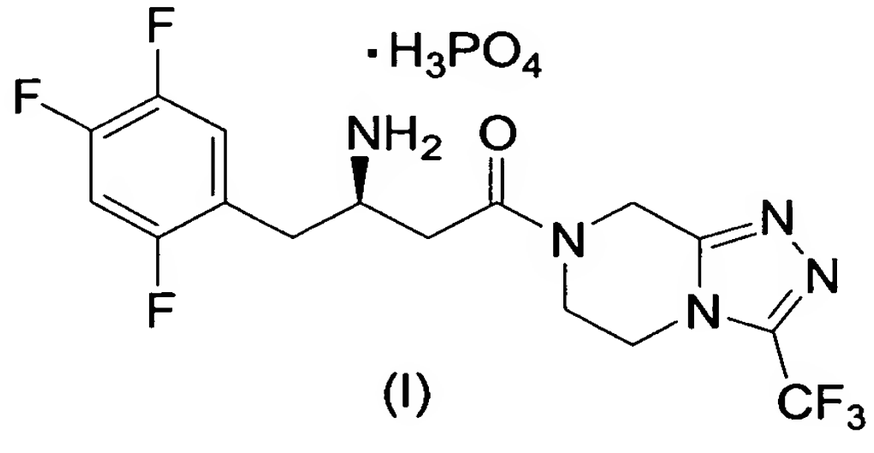

(I)

comprising a detectable amount of crystalline anhydrate Form I or crystalline anhydrate Form III or a mixture thereof.

48. (original) A dihydrogenphosphate salt of (2*R*)-4-oxo-4-[3-(trifluoromethyl)-5,6-dihydro[1,2,4]triazolo[4,3-*a*]pyrazin-7(8*H*)-yl]-1-(2,4,5-trifluorophenyl)butan-2-amine of structural formula I:

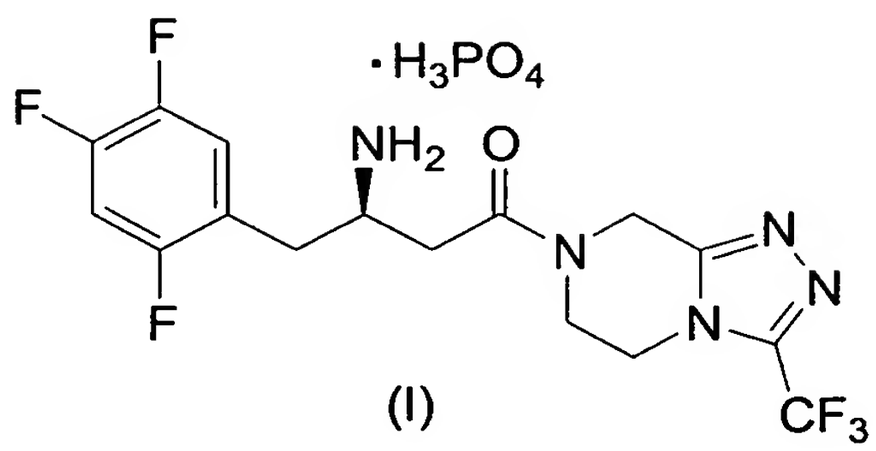

(I)

comprising substantially all by weight of crystalline anhydrate Form I or crystalline anhydrate Form III or a mixture thereof.

49. (currently amended) A pharmaceutical composition comprising a ~~prophylactically or~~ therapeutically effective amount of the salt of Claim 1 or Claim 12 or a mixture thereof in association with one or more pharmaceutically acceptable carriers or excipients.

50. (original) A method of treating Type 2 diabetes comprising administering to a patient in need of such treatment a therapeutically effective amount of the salt according to Claim 1 or Claim 12 or a mixture thereof.

51-52 (cancelled)